RESEARCH ARTICLE

Comparison of Scour and Flow Characteristics Around Circular and Oblong Bridge Piers in Seepage Affected Alluvial Channels

Rutuja Chavan[1] · B. Venkataramana[1] · Pratik Acharya[1] · Bimlesh Kumar[1]

Abstract

The present study examines scour geometry and turbulent flow characteristics around circular and oblong piers in alluvial channel with downward seepage. Experiments were conducted in plane sand bed of non-uniform sand under no seepage, 10% seepage and 15% seepage conditions. Scour depth at oblong pier is significantly lesser than the scour depth at circular one. However, the scour depth at both piers reduces with downward seepage. The measurements show that the velocity and Reynolds stresses are negative near the bed at upstream of piers where the strong reversal occurs. At downstream of oblong pier near the free surface, velocity and Reynolds stresses are less positive; whereas, they are negative at downstream of circular pier. The streamline shape of oblong pier leads to reduce the strength of wake vortices and consequently reversal flow at downstream of pier. With application of downward seepage turbulent kinetic energy is decreasing. The results show that the wake vortices at oblong pier are weaker than the wake vortices at circular pier. The strength of wake vortices diminishes with downward seepage. The Strouhal number is lesser for oblong pier and decreases with downward seepage for both oblong and circular piers.

Keywords Downward seepage · Oblong pier · Scour · Strouhal number · Turbulent kinetic energy

1 Introduction

Scour is removal of sediment particles around the structures constructed in flowing stream due to erosive action of flowing stream such that there is tendency to expose the foundation of structure which may result in structural collapse. Scour at a pier is caused due to the forces exerted on the bed by the complex, highly three-dimensional and unsteady flow field generated by the pier (Kirkil et al. 2009). Scour is a worldwide phenomenon and of great concern especially to civil engineers as any structure constructed in a flowing stream, will have a tendency to advance scour around pier due to a sudden change in the flow pattern. Statistical studies of last few decades show that scour around bridge piers is major reason behind major damage to bridges which endangers lives of travelling public and disruption to heavy traffic. Since 1950 in the USA, 60% of 823 bridges have been damaged or collapsed as a result of river bed scour (Shirhole and Holt 1991). According to their

✉ Bimlesh Kumar
bimk@iitg.ernet.in

1   Department of Civil Engineering, Indian Institute of Technology
      Guwahati, Guwahati 781039, India

study, US Federal Highway Association reported that every year about 50 bridges fail in the USA and out of which 50% bridges failed due to scour around piers and noted that damage to bridges and highway cost US$100 million per year. Thus, scour is major cause of bridge failure. Many researchers have conducted laboratory experiments to predict the scour depth around piers and to study scour mechanism (Laursen and Toch 1956; Breusers et al. 1977; Melville and Sutherland 1988; Kothyari et al. 1992; Melville and Coleman 2000; Chang et al. 2004). Some of the investigators have studied the evolution of scour depth the scour depth in uniform sediment under steady flow condition (Ettema 1980; Yanmaz and Altinbilek 1991; Melville and Chiew 1999). Some researchers have found out effect of sediment gradation on scour depth with non-uniform sand (Ettema 1980; Raudkivi and Ettema 1983; Melville and Sutherland 1988; Kothyari et al. 1992; Oliveto and Hager 2002). Kothyari et al. (1992) have concluded that with increase in standard deviation of sediment gradation the scour depth decreases. Most of the researchers have focused on the horseshoe vortex forming at upstream of pier as it was thought to be responsible for growth of scour around piers (e.g. Melville and Coleman 2000). The flow separation at upstream of piers results in formation of wake vortices at downstream of piers, the strength of wake vortices to erode

the bed material is drastically reducing with the distance because of which eroded bed material get deposited at downstream of piers (Richardson and Davies 1995). In addition, the sediment transportation is complex phenomenon due to interaction of many parameters as it leads to change the bed morphology (Bennett and Nordin 1977; Karim and Holly 1986; Lee and Odgaard 1986). Consequently, the changes in river morphology significantly affects fish communities or aquatic habitats in rivers as they are quite sensitive to availability of stable pools and scour volume (Arlinghaus et al. 2002; Armstrong et al. 2003).

The vortex system around pier, which consists of horseshoe vortex at upstream of pier, wake vortices at downstream of pier, trailing vortices and bow wave is depending upon size and shape of piers (Al-Shukur et al. 2016). Jueyi et al. (2010) have conducted laboratory experiments to compare scour depth around semi-elliptical and semi-circular abutments with armoured beds. The researchers have found that the scour depth at semi-elliptical abutment is lesser than the scour depth at semi-circular abutments. Al-Shukur et al. (2016) have carried out experimental investigation using ten different shapes of piers and found that scour depth is minimum for streamline shapes where maximum for rectangular pier. As scour around piers is result of complex interaction between turbulent flow and bed material so, study of turbulent flow statistics around piers gives more insight in the process of scouring (Ahmed and Rajaratnam 1998). In this study, two shapes of pier namely, oblong and circular piers are used and the study focuses on effect of shape pier on turbulent flow characteristics and bed geometry around piers.

Generally, natural streams are made up of permeable boundaries, which allows water to flow in or out from boundaries. Depending upon the level of surrounding ground water table, water seeps into (upward seepage) and out (downward seepage) from the channel. The interaction between main channel flow and ground water is very important as it plays vital role in controlling the transport of contaminants and maintaining a healthy stream ecosystem (Brunke and Gonser 1997; Jones and Mulholland, 1999). Sharma and Chawla (1975) estimated seepage losses of 45% of the water supplied at head of the channel. Krishnamurthy and Rao (1969) have reported seepage losses of 2.2 m^3 per day per length in Ganga canal. Seepage losses of 20%–50% of the total flow, in unlined canal in semi-arid region have been evaluated by Tanji and Kielen (2002). Kinzli et al. (2010) estimated around 40% losses due to downward seepage. Martin and Gates (2014) evaluated water loss around 15% upstream flow rate due to downward seepage. In addition to losses, downward seepage is responsible for change in bed condition and sediment transport in the channel. Many researchers have found out that downward seepage may alter channel geometry, increase the Reynolds shear stresses near the boundary and consequently enhance the sediment motion. (Rao et al. 2011; Patel et al. 2015; Deshpande and Kumar 2016). Qi et al. (2012) have carried out experiments to

investigate effect of seepage on scour depth around circular pier, with 2% downward seepage and found a reduction in equilibrium scour depth. Similarly, Soltani-Gerdefaramarzi et al. (2013 and 2014) have conducted laboratory experiments with a combined system of bed suction and jet injection through the pier body and found that suction and injection together results in reduction of scour depth. Cao and Chiew (2014) has also shown that sediment transport rate increases with the increase in length of the suction zone. Thus in the present study, downward seepage was applied throughout the length of the channel with alluvial streambed to imitate the natural pattern of suction up to a certain extent. The study of seepage flows is important to understand its effect on detachment and further transportation of bed material as transportation of sediment results in aggradation and degradation of channel boundaries. For management of fluvial system, it is necessary to understand the phenomenon of sediment transport. Thus, this study is related to the solution of important practical engineering problems as ground water movement have to consider while constructing hydraulic structures like bridge piers. In this study, comparison between flow characteristics and scour around oblong and circular pier has been done with incorporating downward seepage parameter.

2 Experimental Set-Up and Methodology

Experiments were conducted in a glass-walled tilting flume of length 17.2 m, 1-m width and 0.72-m depth. The basic details of experimental set-up can be obtained from Chavan et al. (2017) (Fig. 1).

In this study, two types of piers were used, i.e. circular and oblong piers. Diameters of circular pier was 75 mm; whereas, oblong pier of width 75 mm, length 225 and 270 mm were used. Height of piers was 150 mm. The sizes of piers were selected in such a way that width of pier should not be greater than 10% of channel width to avoid side wall effect on scour depth (Chiew and Melville 1987). The bed slope was fixed at 0.05%. First the sand bed was prepared plane throughout the channel. Thickness of sand bed was 17 cm in all experimental runs. Then piers were installed at 7.5 m, i.e. at centre of the test section of 5 to 10 m from downstream end of flume in such a way that the approach length ought to fulfil the fully developed flow condition. As riverbed are comprising of non-uniform sediment particles (Wu et al. 2004), the experiments were carried out in the sand bed made up of non-uniform sand of median size (d50) 0.5 mm. The geometric standard deviation (σg) for selected sand is 1.65, i.e. greater than 1.4 which confirms non-uniformity of sand (Marsh et al. 2004). Further, as far as the flow is concerned, considering to the fact that the aspect ratios were greater than 6, the flows in the experiments were free from 3D (three dimensional) effect provided by the side-walls (Yang et al. 2004). Experiments were conducted for
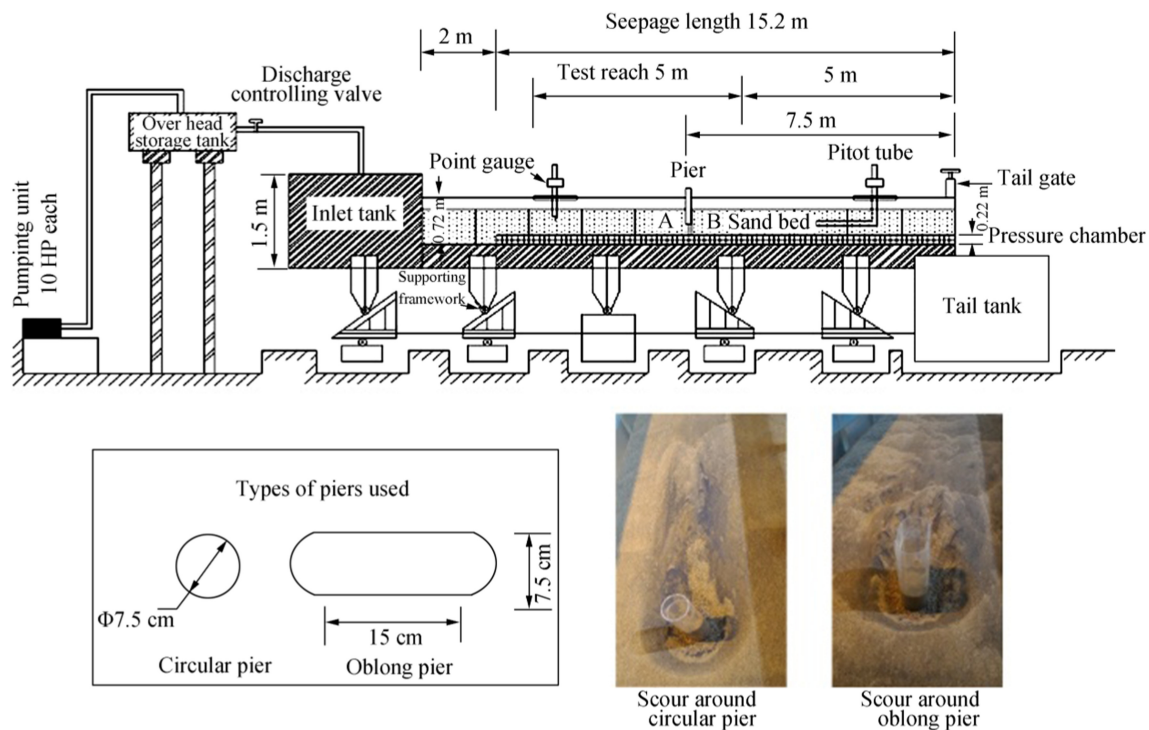
Fig. 1 Experimental set-up

three different discharges and for each discharge 10% seepage and 15% seepage were applied. Experimental runs were conducted for 24 h. Experimental conditions for present study are shown in Table 1.

Ultrasonic ranging system (SeaTek®) was used to measure the bed geometry, which is consisting of four pairs of transducers. The SeaTek instrument measures the distance to a target of wavelength 0.3 mm in water with 5 MHz ultrasound with measurement accuracy of 0.1 mm. Acoustic Doppler velocimeter (ADV) was used to take velocity measurements around piers. Velocity measurements were taken at 20 different depths within the flow depth for 5 min at each depth. The sampling rate used for collecting data was 200 Hz. ADV works with 10-MHz acoustic frequency and has precision of

millimeter. Time averaged velocity in streamwise direction (u) and in vertical direction (w) are defined as:

$$u = \frac{1}{N} \sum_{i=1}^{N} U_i \tag{1}$$

$$w = \frac{1}{N} \sum_{i=1}^{N} W_i \tag{2}$$

where U_i and W_i are instantaneous velocities in streamwise direction and vertical direction respectively. N is number of instantaneous velocity samples. Fluctuating components in streamwise (u') and vertical direction (v') are obtained by:

$$u' = U_i - u \tag{3}$$

Table 1 Details of experimental conditions

Sr. no.	Flow depth (h) /m	Discharge (Q) /(m³·s⁻¹)	Reynolds no.	Froude no.	% of seepage
1	0.118	0.032	32 000	0.25	0
					10
					15
2	0.123	0.036	36 000	0.264	0
					10
					15
3	0.129	0.04*	40 000	0.275	0
					10
					15

* Turbulent analysis has been performed for this observation

$$w' = W_i - w \tag{4}$$

Reynolds shear stress are calculated as:

$$\tau_{uw} = -\overline{\rho u' w'} \tag{5}$$

The velocity data measured by the ADV is post processed by acceleration threshold method (Goring and Nikora 2002) to remove spikes included due to interference between transmitted and received signals. To fit the velocity power spectra with Kolmogorov's -5/3 law in the inertial subrange (Devi and Kumar 2015), the threshold values have been chosen between 1 to 1.5 by trial and error method. Average correlation coefficient between transmitted and received signal is less than 70% and signal to noise ratio (SNR) kept between 10 and 15.

3 Results and Discussions

3.1 Bed Geometry Around Piers

Figures 2 and 3 show contour of bed morphology around oblong and circular piers respectively for no seepage, 10% seepage and 15% seepage conditions. It can be observed from Figs. 2 and 3 that the scoured region is large for circular pier than oblong pier. The scour depth at oblong pier is reduced by 15% than the scour depth at circular pier under the same experimental conditions. The diameter of scour hole is more in case of circular pier than oblong pier and that too for every experimental condition. However, the deposition height and deposition length at downstream of pier is also greater for circular pier.

Scouring around piers is time depending phenomenon. Scour depth at piers is increasing gradually with increasing time. After a certain limit, equilibrium sets between erosive capacity of flowing stream and extent of bed material to get erode. Figure 4 shows graph of scour depth with respect to time. From Fig. 4, it can be observed that the scour depth is increasing with increase in time; however, rate of increase of scour depth is more in no seepage runs than in seepage runs (Chavan et al. 2017). Initially the rate of increase of scour depth is more and reduces gradually with increase in time such that, nearly after 12 h, equilibrium condition is reached.

The scoured bed material is deposited at downstream of piers along and at sides of centreline. Figure 5 shows bed elevation along the centreline in longitudinal direction. Close observation of Fig. 5 shows that scour depth at upstream of pier is lesser for oblong pier than circular pier in all experimental conditions. However, scour depth at oblong pier is more in case of no seepage condition and reduced by 15% in case of 10% seepage condition and again reduced by 25% for 15% seepage condition. Similarly, for circular pier in case of 10% seepage and 15% seepage conditions, the scour depth
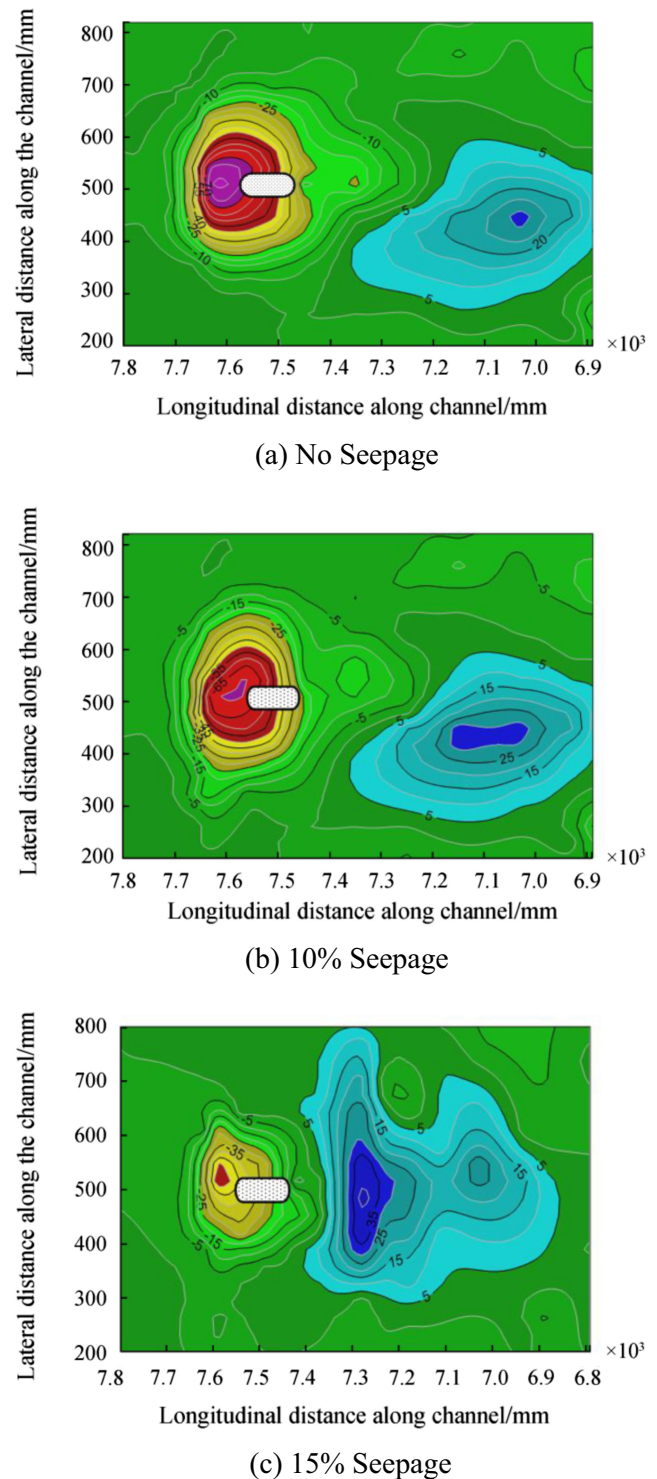

(a) No Seepage

(b) 10% Seepage

(c) 15% Seepage

Fig. 2 Contour diagram of scour around oblong pier (scour depth in mm)

is reduced by 17% and 29%, respectively. The scoured bed material is deposited further at downstream of pier along and at sides of the centreline and produce hump at rear side of pier. For both shapes of pier, the height of deposition is increased with increased seepage percentage. At downstream of oblong

(a) No Seepage
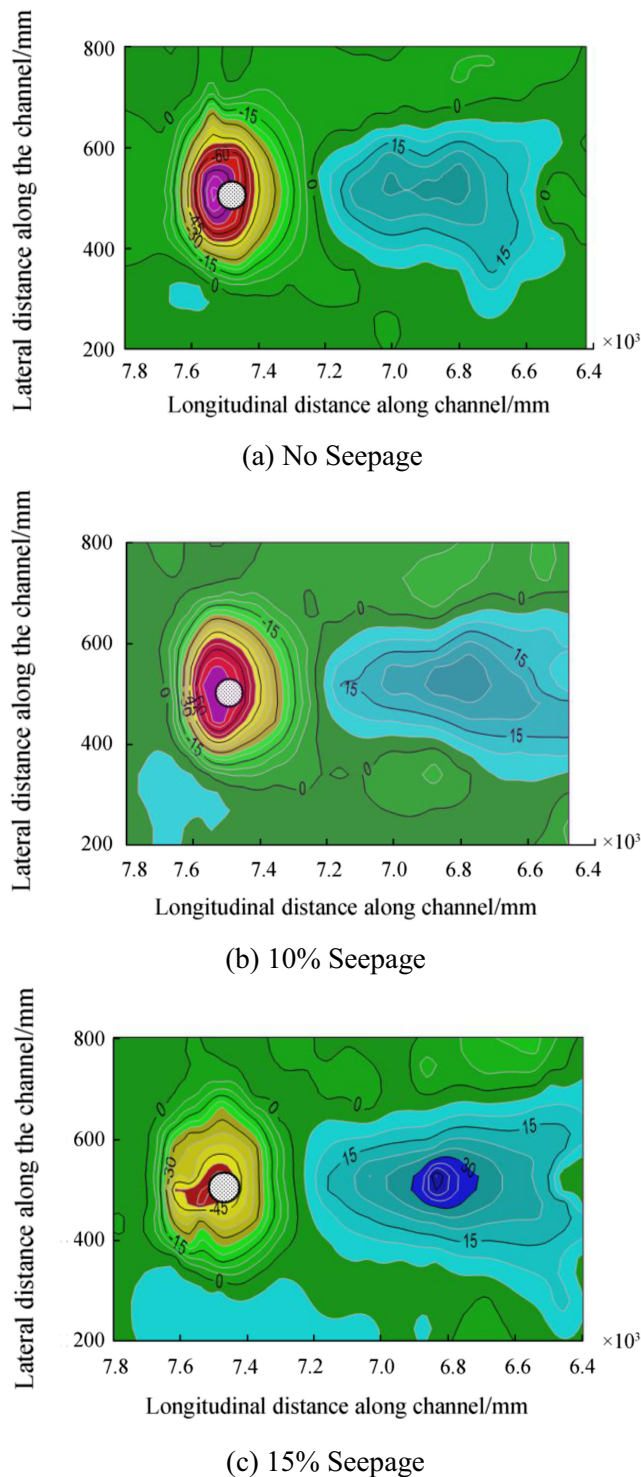

(b) 10% Seepage

(c) 15% Seepage

Fig. 3 Contour diagram of scour around circular pier (scour depth in mm)

pier, height of deposition is increased by 30% in case of 10% seepage condition and again increased by 50% in case of 15% seepage. For circular pier, deposition height is increase by 32% on application of 10% seepage and 70% in case of 15% seepage. With time, the vortex around pier increased in longitudinal and lateral direction too.
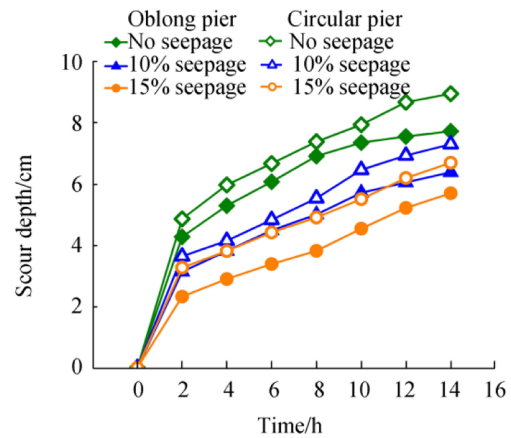

Fig. 4 Development of scour depth with time at oblong pier and circular pier

Figure 6 shows lateral bed profile at upstream of oblong and circular pier for no seepage, 10% seepage and 15% seepage condition. Close observation of Fig. 6 shows that depth of scour hole at upstream of piers are decreasing with downward seepage; however, width of scour hole is increasing with increase in downward seepage. For circular pier, width of scour hole is increased in 10% seepage run by 25% and again increased by 36% in 15% seepage run. For oblong pier, scour hole width is increased by 28% in case of 10% seepage condition and again increase by 44% for 15% seepage condition. From Fig. 6, it is also observed that, width of scour hole is lesser for oblong pier than circular pier. The percentage reduction of scour characteristics in oblong pier than circular pier is mentioned in Table 2.

As the shape of pier plays an important role in scouring around pier, so in this study, it is observed that oblong shape of pier can be protecting measure against scour in comparison with circular one. However, for both of the shapes of pier the scour depth is reducing with application of downward seepage.

3.2 Velocity

The velocity measurements were taken by ADV at upstream and downstream of pier which are the most critical sections as
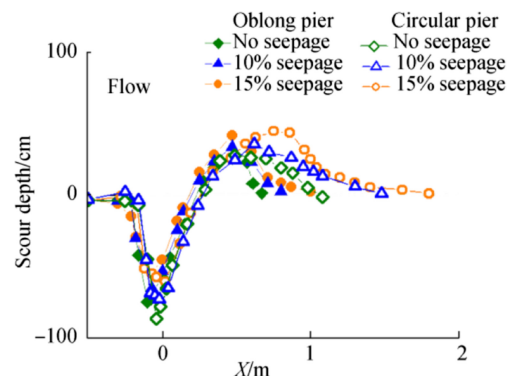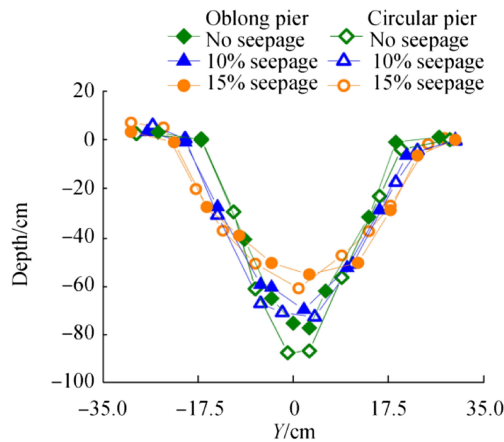

Fig. 5 Bed profile along the centre line at oblong pier and circular pier

Fig. 6 Lateral bed profile at upstream of oblong pier and circular pier

upstream and downstream sections are the most affected sections due to flow separation around pier. For oblong pier, measurements were taken at upstream A (7.6725, 0.5) and downstream B (7.3275, 0.5) and for circular pier, at upstream A (7.5975, 0.5) and downstream B (7.4025, 0.5).

Figure 7a, b shows comparison between time averaged velocity in streamwise direction for no seepage and seepage runs for both oblong and circular piers respectively. From Fig. 7, it can be seen that the trend of velocity profile at upstream section is same for both oblong and circular piers. Stremwise velocity is negative near the bed at upstream of piers (Fig. 7) as the downflow at face of piers hits the bed, it moves in reverse direction to that of streamflow. Due to reversal flow near the bed at upstream of pier, stremwise velocity is found to be negative. With application of downward seepage, the reversal velocity is decreasing. From Fig. 7, it can be observed that the reversal velocity near the bed is more in no seepage runs and lessens for 10% seepage and again decrease in case of 15% seepage runs. The decrement in reversal velocity at upstream section is in agreement with literature (Chavan et al. 2017; Chavan and Kumar 2017). At upstream of pier, the downward seepage impedes the reversal flow; hence, the velocity near the bed at upstream of pier is decreasing with application of downward seepage. At downstream of pier, reversal flow can be found near free surface due to wake vortices forming at downstream of pier. At downstream

section of circular pier, streamwise velocity is negative near free surface then increasing gradually with moving towards bed (Izadinia et al. 2013). With downward seepage, reversal velocity near free surface is decreasing whereas near the bed, velocity is increasing with increasing seepage percentage. While flow separation at upstream of oblong pier, the flow becomes streamline while moving along the sides of pier which results in diminishing the strength of wake vortices at downstream of oblong pier. So at downstream of oblong pier, near the free surface the velocity is less positive unlike the circular pier.

3.3 Reynolds Shear Stress

The approaching streamflow is obstructed by pier and results in flow separation in the form of downflow at upstream face of pier and side circulations along the sides of pier. The change in streamflow pattern results in increasing Reynolds shear stress and consequently scouring around pier. Figure 8 shows distribution of Reynolds shear stress along the flow depth for no seepage, 10% seepage and 15% seepage condition. At upstream of both oblong and circular piers, Reynolds shear stress is found to be negative near the bed region and near free surface at downstream of circular pier. Reynolds shear stress is decreasing with downward seepage at upstream of pier near the bed and near free surface at downstream of both piers. At downstream of pier Reynolds shear stress is fluctuating heavily, due to irregular wake vortices. However, fluctuations in Reynolds stress are more at downstream of circular pier than at downstream of oblong pier due to stronger wake vortices.
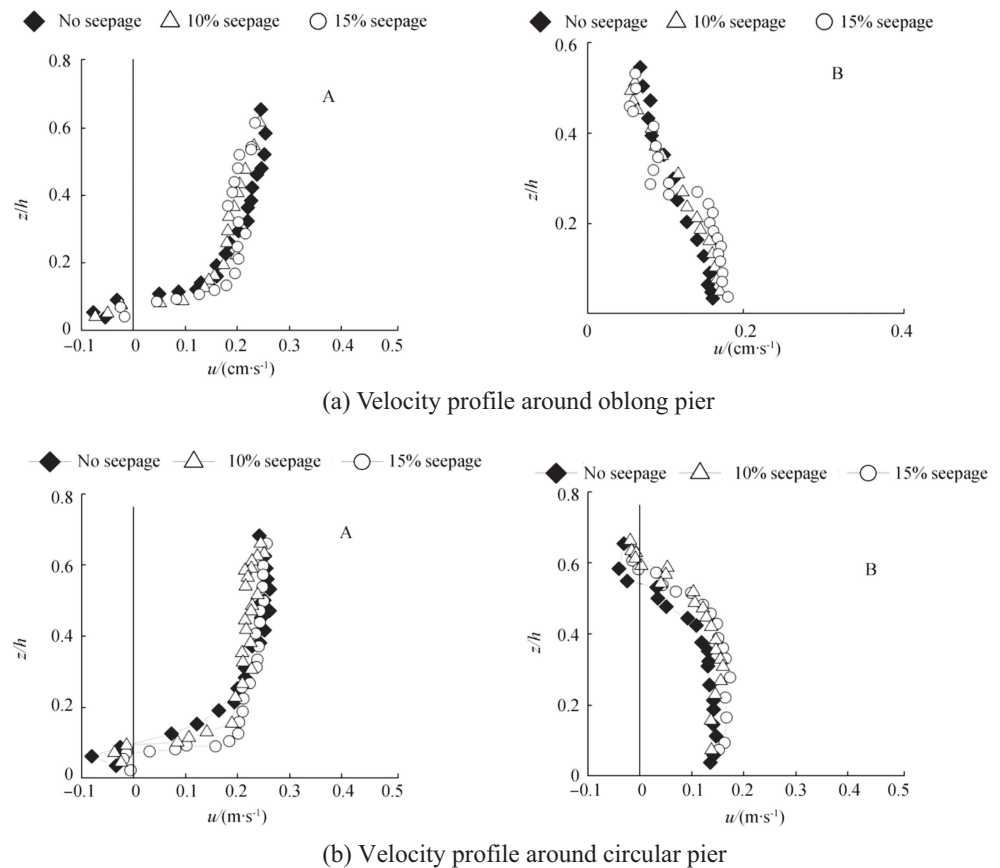
3.4 Turbulent Kinetic Energy

Vertical profile of turbulent kinetic energy (TKE) $\frac{\rho}{2}\left(\overline{u'^2} + \overline{v'^2} + \overline{w'^2}\right)$ at upstream (A) and downstream (B) of oblong pier and circular pier for no seepage, 10% seepage and 15% seepage runs are depicted in Fig. 9a, b. From Fig. 9, it can be seen that TKE is highly fluctuating due to flow separation. At upstream of both piers, TKE is lesser near free surface and increasing gradually away from free surface attends maximum value near the edge of scoured region and again decreasing towards bed. At upstream section near the bed region, magnitude of TKE is more for no seepage condition and decreasing with increasing seepage percentage as downward seepage lessens the strength of reversal flow which results in decrement of TKE. (Chavan and Kumar 2017). Separation of flow and strong pressure gradient at upstream of pier leads to enhance kinetic energy at the edge of scour hole and consequently increase the rate of scouring (Maity and Mazumder 2012). At downstream section (B), TKE is fluctuating heavily, having maximum value near free surface and

Table 2 Table showing % difference of scour characteristics between circular and oblong piers

Scour characteristics	% reduction for oblong pier		
	No seepage	10% seepage	15% seepage
Scour depth	15	13	13
Scour width	21	22	20
Deposition height	7.5	6.8	7.2
Deposition length	52	55.6	49

Fig. 7 Velocity profiles around **a** oblong pier and **b** circular pier at sections (A) upstream A, (B) downstream B

(a) Velocity profile around oblong pier

(b) Velocity profile around circular pier

then decreasing with moving towards bed. The TKE fluctuations and magnitude of TKE are significantly higher at downstream of circular pier.
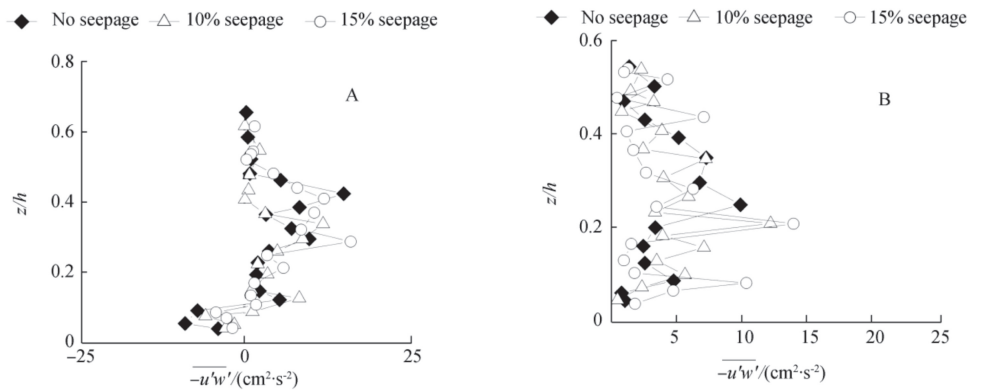
3.5 Power Spectra Analysis

Power spectrum analysis of instantaneous velocity measurements has been carried out at wake region of piers to find out intensity of wake vortices. Power spectra were calculated from fast Fourier transformation (FFT) of auto-covariance function of velocity time series data. The resultant power spectra is obtained from, $S(f) = \{S_u(f)^2 + S_v(f)^2 + S_w(f)^2\}^{0.5}$ where, $S_u(f)$, $S_v(f)$ and $S_w(f)$ are power spectra of velocity components in streamwise, transverse and vertical direction.

Figure 10 shows resultant power spectra against frequency at downstream of piers for no seepage, 10% seepage and 15% seepage runs. In the power spectrum, distribution at a certain point, the peak frequency related to power that demonstrates strength of wake vortices at that point. The strength of wake vortices indicates the ability of wake vortices to entrain and move the bed particles. Strouhal number (fD/U_0) is calculated from power spectra analysis, where, f is vortex shedding frequency; which is associated with maximum $S(f)$ in Fig. 10, D is hydraulic diameter of pier and U_0 is depth average flow velocity. The values of Strouhal number, near free surface
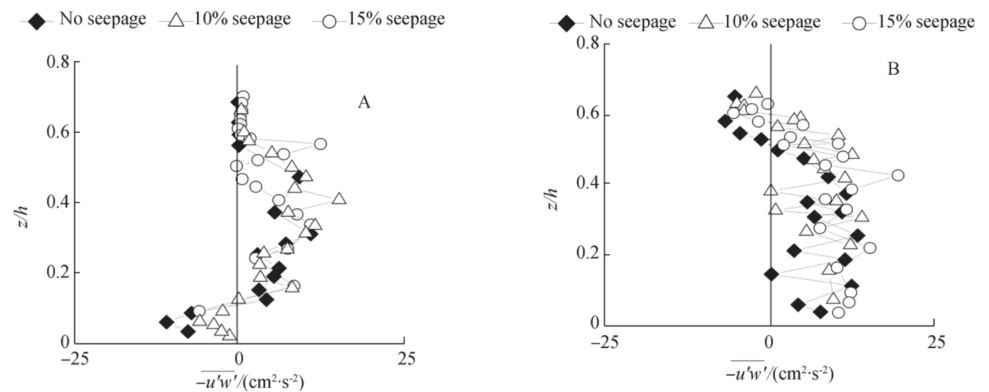
and near the bed region for all experimental conditions for both oblong and circular piers are prescribed in Table 3.

For circular pier, for no seepage condition, the Strouhal number near free surface is 0.23 which is comparable with present literature (Igarshi 1981; Sumner et al. 1999; Ataie-Ashtiani and Aslani-Kordkandi 2013; Chavan and Kumar 2017). Near the bed, i.e. within the scour hole the value of Strouhal number is lesser which shows that the strength of wake vortices is lesser near the bed and increases away from the bed (Ataie-Ashtiani and Aslani-Kordkandi 2013). From Table 2, it can be observed that, Strouhal number is lesser in case of oblong pier and more for circular pier. Strength of vorticity is more at downstream of circular pier than oblong pier. However, with application of downward seepage strength of wake vortices is decreasing for both circular and oblong piers. Comparing both oblong and circular piers, the wake of oblong pier is quite weaker than circular pier which indicates that the capacity of wake vortices to scour the bed material at downstream of oblong pier is lesser than the capacity of wake vortices at downstream of circular pier. In case of oblong pier as the flow hits the pier, it separates in the form of downflow along upstream face of pier and side circulations along sides of pier. The sides of oblong pier are straight unlike the circular pier, which curtails the turbulence at sides of pier and make the flow streamline. When this streamlined flow

Fig. 8 RSS profiles around **a** oblong pier and **b** circular pier at sections (A) upstream A, (B) downstream B
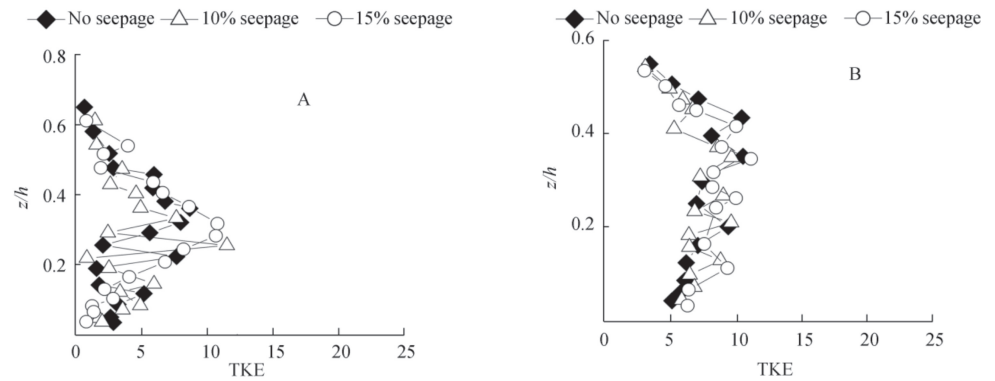

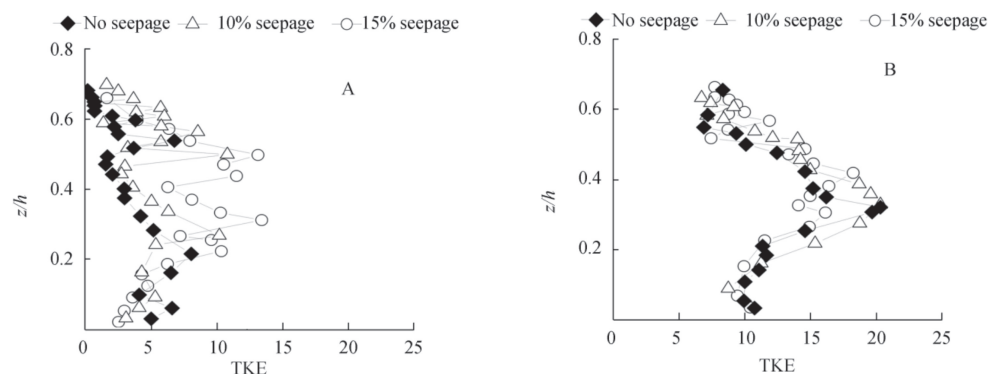(a) RSS profile around oblong pier

(b) RSS profile around circular pier

Fig. 9 Vertical distribution of turbulent kinetic energy at **a** oblong pier and **b** circular pier at sections (A) upstream A, (B) downstream B
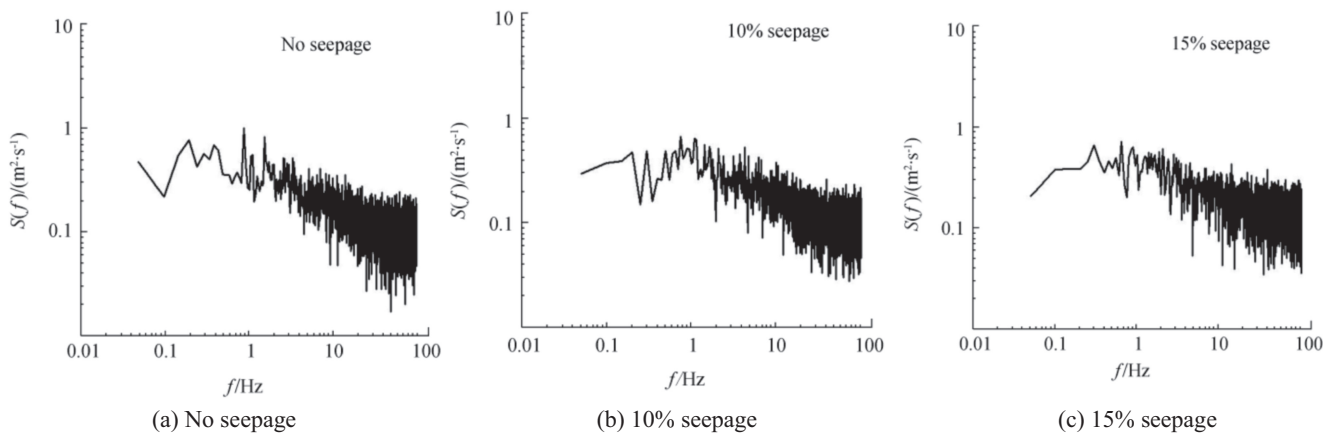

(a) TKE profile around oblong pier

(b) TKE profile around circular pier

(a) No seepage   (b) 10% seepage   (c) 15% seepage

Fig. 10 Power spectra at downstream of oblong pier

reached at downstream of pier it creates lesser turbulence because of which the strength of wake vortices is reduced at downstream of oblong pier. The capacity of wake vortices to erode the bed material at downstream of both oblong and circular piers, diminishes with application of downward seepage.

4 Discussions

Present results highlight the inclusion of seepage in the analysis or design of the piers. Rivers, streams or irrigation channels often comprise of porous boundaries made up of sediment particles or gravel beds. An essential and well-known feature of permeable boundaries is that mass and momentum transfer takes place across the interface between the fluid and porous media. Thus, flow in natural channels is a complex interaction between surface and subsurface flow. Water is continuously seeping in (upward seepage) or out (downward seepage) from channel bed and banks depending upon the difference in level of water between channel and surrounding ground water table. Because of presence of seepage through porous boundaries, additional hydrodynamic forces may be exerted on sediment particles. These additional forces may have significant impact on sediment transportation. Thus, presence of seepage leads to change bed morphology and hydrodynamics characteristics of alluvial channels. Results have shown that with downward seepage, scour depth at

upstream of the piers reduces, consequence of which cost of protection measures may come down if seepage is included in the design. A proper inclusion of seepage as design variable may help in mitigating the downstream deposition of sediment at rear side of pier. The downstream deposition generally forms a dune like structure, which offers more resistance to flow and thereby reducing the conveyance capacity of the channel. This may have negative impact on navigation and flora-fauna, which comes from the present experimental observations.

The important aspect of present experimental observation is about geometric shape of the pier, which greatly affects the formation and characteristics of the scour hole pattern. The oblong shape prevents the early flow separation and thus has a positive effect on scour hole formation and its geometric features. Based on the present experiments, it can be said that oblong shape is well suited as piers and also seepage must be considered in the analysis and design of the pier.

5 Conclusions

Experiments were conducted in tilting flume to compare scour and turbulent flow statistics around circular and oblong bridge piers in seepage affected alluvial channel. Flume experiments were done with no seepage, 10% seepage and 15% seepage conditions for three different discharges using circular and oblong piers. Various results showing distribution of velocity, Reynolds stress, turbulent kinetic energy, power spectra analysis and bed morphology after scouring around circular and oblong piers are presented for no seepage, 10% seepage and 15% seepage conditions. Following are the conclusions drawn from present study:

(1) The scour depth at circular pier is found to be more than the scour depth at oblong pier. The width of scour hole is also more in case of circular pier. The scoured bed material is carried by flowing stream and deposited at

Table 3 Strouhal number at downstream of piers

Case	Circular pier		Oblong pier	
	Near free surface	Near bed	Near free surface	Near bed
No seepage	0.23	0.14	0.22	0.12
10% seepage	0.20	0.12	0.19	0.10
15% seepage	0.18	0.11	0.16	0.08

downstream of pier. The extent of deposited bed material is more at downstream of circular pier. So oblong bridge pier can be used instead of circular bridge pier as protecting measure against scour. With application of downward seepage, scour depth is reducing for both the piers. However, width of scour hole and deposition height at downstream of piers are increasing with increasing downward seepage for both types of piers.

(2) Strong reversal flow has been observed at upstream of both piers, near the bed region. The wake vortices at downstream of oblong piers are weaker than the wake vortices at circular pier. In case of seepage runs, for both the pies, the reversal velocity decreases. At upstream of both piers, in case of 10% seepage the reversal velocity near bed decreases and again reduces for 15% seepage. At downstream of both piers, in case of seepage runs velocity decreases near free surface however, it increases near bed.

(3) Reynolds shear stress at upstream of both piers is negative near bed and decreases with downward seepage. At downstream of circular pier, Reynolds stresses are negative near free surface and changes to positive away from free surface. At downstream of both piers, near free surface Reynolds stresses are decreasing on application of downward seepage. At downstream of both piers Reynolds stresses fluctuates heavily due to irregular wake vortices. However, magnitude of Reynold stresses is more at downstream of circular pier due to stronger wake of circular pier.

(4) Turbulent kinetic energy is more for no seepage condition, for both piers and reduces on application of downward seepage which indicates the reduction in strength of flow to scour the bed material. Turbulent kinetic energy is higher for circular pier than oblong pier.

(5) Lesser Strouhal number for oblong pier indicates lesser capacity of wake vortices at to scour the bed material. Strouhal number is decreasing with increasing downward seepage for both the piers which suggest that downward seepage diminishes the strength and consequently erosive capacity of wake vortices.

References

Ahmed F, Rajaratnam N (1998) Flow around bridge piers. J Hydraul Eng 124(3):288–300. https://doi.org/10.1061/(ASCE)0733-9429(1998)124:3(288)

Al-Shukur AHK, Obeid ZH (2016) Experimental study of bridge pier shape to minimize local scour. Int J Civil Eng Technol 7(1):162–171

Arlinghaus R, Engelhardt C, Sukhodolov A, Wolter C (2002) Fish recruitment in a canal with intensive navigation: implications for ecosystem management. J Fish Biol 61(6):1386–1402. https://doi.org/10.1111/j.1095-8649.2002.tb02484.x

Armstrong JD, Kemp PS, Kennedy GJA, Ladle M, Milner NJ (2003) Habitat requirements of Atlantic salmon and brown trout in rivers and streams. Fish Res 62(2):143–170. https://doi.org/10.1016/S0165-7836(02)00160-1

Ataie-Ashtiani B, Aslani-Kordkandi A (2013) Flow field around single and tandem piers. Flow, Turbul Combust 90(3):471–490. https://doi.org/10.1007/s10494-012-9427-7

Bennett JP, Nordin CF (1977) Simulation of sediment transport and armouring/simulation des transports solides et de l'armure du lit. Hydrol Sci J 22(4):555–569. https://doi.org/10.1080/02626667709491760

Breusers HNC, Nicollet G, Shen HW (1977) Local scour around cylindrical piers. J Hydraul Res 15(3):211–252. https://doi.org/10.1080/00221687709499645

Brunke M, Gonser TOM (1997) The ecological significance of exchange processes between rivers and groundwater. Freshw Biol 37(1):1–33. https://doi.org/10.1046/j.1365-2427.1997.00143.x

Cao D, Chiew YM (2014) Suction effects on sediment transport in closed-conduit flows. J Hydraul Eng 140(5):04014008. https://doi.org/10.1061/(ASCE)HY.1943-7900.0000833

Chang WY, Lai JS, Yen CL (2004) Evolution of scour depth at circular bridge piers. J Hydraul Eng 130(9):905–913. https://doi.org/10.1061/ASCE!0733-9429~2004!130:9~905

Chavan R, Kumar B (2017) Experimental investigation on flow and scour characteristics around tandem piers in sandy channel with downward seepage. J Mar Sci Appl 16(3):313–322. https://doi.org/10.1007/s11804-017-1426-6

Chavan R, Sharma A, Kumar B (2017) Effect of downward seepage on turbulent flow characteristics and bed morphology around bridge piers. *J Mar Sci Appl* 16(1):60–72. https://doi.org/10.1007/s11804-017-1394-x

Chiew YM, Melville BW (1987) Local scour around bridge piers. J Hydraul Res 25(1):15–26. https://doi.org/10.1080/00221688709499285

Deshpande V, Kumar B (2016) Turbulent flow structures in alluvial channels with curved cross-sections under conditions of downward seepage. Earth Surf Process Landf 41(8):1073–1087. https://doi.org/10.1002/esp.3889

Devi TB, Kumar B (2015) Turbulent flow statistics of vegetative channel with seepage. J Appl Geophys 123:267–276. https://doi.org/10.1016/j.jappgeo.2015.11.002

Ettema R (1980) Scour at bridge piers. Rep. No. 216, School of Engineering, Univ. of Auckland, Auckland, New Zealand

Goring DG, Nikora VI (2002) Despiking acoustic Doppler velocimeter data. J Hydraul Eng 128(1):117–126. https://doi.org/10.1061/(ASCE)0733-9429(2002)128:1(117)

Igarashi T (1981) Characteristics of the flow around two circular cylinders arranged in tandem: 1st report. Bull JSME 24(188):323–331. https://doi.org/10.1299/jsme1958.24.323

Izadinia E, Heidarpour M, Schleiss AJ (2013) Investigation of turbulence flow and sediment entrainment around a bridge pier. Stoch Env Res Risk A 27(6):1303–1314. https://doi.org/10.1007/s00477-012-0666-x

Jones, J. B., & Mulholland, P. J. (1999). Streams and ground waters. Academic press

Jueyi S, Hossein A, Abdolreza K, Samani A, Mehrnoosh M (2010) Clear-water scour around semi-elliptical abutments with armored beds. Int J Sediment Res 25:233–245. https://doi.org/10.1016/S1001-6279(10)60041-8

Karim MF, Holly FM Jr (1986) Armoring and sorting simulation in alluvial rivers. J Hydraul Eng 112(8):705–715. https://doi.org/10.1061/(ASCE)0733-9429(1986)112%3A8(705)

Kinzli KD, Martinez M, Oad R, Prior A, Gensler D (2010) Using an ADCP to determine canal seepage loss in an irrigation district. Agric Water Manag 97(6):801–810. https://doi.org/10.1016/j.agwat.2009.12.014

Kirkil G, Constantinescu G, Ettema R (2009) Detached eddy simulation investigation of turbulence at a circular pier with scour hole. J

Hydraul Eng 135(11):888–901. https://doi.org/10.1061/(ASCE)HY.1943-7900.0000101

Kothyari UC, Garde RCJ, Ranga Raju KG (1992) Temporal variation of scour around circular bridge piers. J Hydraul Eng 118(8):1091–1106. https://doi.org/10.1061/(ASCE)0733-9429(1992)118:8(1091)

Krishnamurthy K, Rao S (1969) Theory and experiment in canal seepage estimation using radioisotopes. J Hydrol 9(3):277–293. https://doi.org/10.1016/0022-1694(69)90022-5

Laursen EM, Toch A (1956) Scour around bridge piers and abutments, vol 4. Iowa Highway Research Board, Ames

Lee HY, Odgaard AJ (1986) Simulation of bed armoring in alluvial channels. J Hydraul Eng 112(9):794–801. https://doi.org/10.1061/(ASCE)0733-9429(1986)112:9(794)

Maity H, Mazumder BS (2012) Contributions of burst-sweep cycles to Reynolds shear stress over fluvial obstacle marks generated in a laboratory flume. Int J Sediment Res 27(3):378–387. https://doi.org/10.1016/S1001-6279(12)60042-0

Marsh NA, Western AW, Grayson RB (2004) Comparison of methods for predicting incipient motion for sand beds. J Hydraul Eng 130(7):616–621. https://doi.org/10.1061/~ASCE!0733-9429~2004!130:7~616

Martin CA, Gates TK (2014) Uncertainty of canal seepage losses estimated using flowing water balance with acoustic Doppler devices. J Hydrol 517:746–761. https://doi.org/10.1016/j.jhydrol.2014.05.074

Melville BW, Chiew YM (1999) Time scale for local scour at bridge piers. J Hydraul Eng 125(1):59–65. https://doi.org/10.1061/(ASCE)0733-9429(1999)125:1(59)

Melville BW, & Coleman SE (2000) Bridge scour. Water Resources Publication

Melville BW, Sutherland AJ (1988) Design method for local scour at bridge piers. J Hydraul Eng 114(10):1210–1226. https://doi.org/10.1061/(ASCE)0733-9429(1988)114:10(1210)

Oliveto G, Hager WH (2002) Temporal evolution of clear-water pier and abutment scour. J Hydraul Eng 128(9):811–820. https://doi.org/10.1061/(ASCE)0733-9429(2002)128:9(811)

Patel M, Deshpande V, Kumar B (2015) Turbulent characteristics and evolution of sheet flow in an alluvial channel with downward seepage. Geomorphology 248:161–171. https://doi.org/10.1016/j.geomorph.2015.07.042

Qi M, Chiew YM, Hong JH (2012) Suction effects on bridge pier scour under clear-water conditions. J Hydraul Eng 139(6):621–629. https://doi.org/10.1061/(ASCE)HY.1943-7900.0000711

Rao AR, Sreenivasulu G, Kumar B (2011) Geometry of sand-bed channels with seepage. Geomorphology 128(3):171–177. https://doi.org/10.1016/j.geomorph.2011.01.003

Raudkivi AJ, Ettema R (1983) Clear-water scour at cylindrical piers. J Hydraul Eng 109(3):338–350. https://doi.org/10.1061/(ASCE)0733-9429(1983)109:3(338)

Richardson, E.V. and Davies, S.R. 1995. "Evaluating scour at bridges".Rep. No. FHWAIP-90-017 (HEC 18), Federal Administration, U.S. Department of Transportation, Washington, D.C.

Sharma HD, & Chawla AS (1975) Manual of canal lining. In Technical Report No. l4. Central Board of Irrigation and Power New Delhi

Shirhole AM, Holt RC (1991) Planning for a comprehensive bridge safety program. Transp Res Rec 1290:39–50

Soltani-Gerdefaramarzi S, Afzalimehr H, Chiew YM, Gallichand J, Ghasemi M (2013) Turbulent characteristics in flow subjected to bed suction and jet injection as a pier-scour countermeasure. Int J Hydraul Eng 2(5):93–100. https://doi.org/10.5923/j.ijhe.20130205.03

Soltani-Gerdefaramarzi S, Afzalimehr H, Chiew YM, Gallichand J (2014) Reduction of pier scour using bed suction and jet injection. Proc Inst Civil Eng, Water Manage 167(2):105–114

Sumner D, Wong SST, Price SJ, Paidoussis MP (1999) Fluid behaviour of side-by-side circular cylinders in steady cross-flow. J Fluids Struct 13(3):309–338

Tanji KK, & Kielen NC (2002) Agricultural drainage water management in arid and semi-arid areas. FAO

Wu B, Molinas A, Julien PY (2004) Bed-material load computations for nonuniform sediments. J Hydraul Eng 130(10):1002–1012

Yammaz AM, Altinbilek HD (1991) Study of time-dependent local scour around bridge piers. J Hydraul Eng 117(10):1247–1268

Yang SQ, Tan SK, Lim SY (2004) Velocity distribution and dip-phenomenon in smooth uniform open channel flows. J Hydraul Eng 130(12):1179–1186